Proceedings of ASME 2011, 5th International Conference on Energy Sustainability & 9th Fuel Cell Science, Engineering and Technology Conference, ESFuelCell2011
August 7-10, 2011, Washington, DC, USA

ESFuelCell2011-54794

Computational Analysis of Heat Transfer in Air-cooled Fuel Cells

S. Shahsavari
Mechatronic Systems Engineering,
School of Engineering Science,
Simon Fraser University, BC,
Canada
sshahsav@sfu.ca

M. Bahrami
Mechatronic Systems Engineering,
School of Engineering Science,
Simon Fraser University, BC,
Canada
mbahrami@sfu.ca

E. Kjeang
Mechatronic Systems Engineering,
School of Engineering Science,
Simon Fraser University, BC,
Canada
ekjeang@sfu.ca

Abstract

Temperature distribution in a fuel cell significantly affects the performance and efficiency of the fuel cell system. Particularly, in low temperature fuel cells, improvement of the system requires addressing the heat management issues, which reveals the importance of developing thermal models. In this study, a 3D numerical thermal model is presented to analyze heat transfer and predict the temperature distribution in air-cooled proton exchange membrane fuel cells (PEMFC). In the modeled fuel cell stack, forced air flow supplies oxidant as well as cooling. Conservation equations of mass, momentum, and energy are solved in the oxidant channel, whereas energy equation is solved in the entire domain, including the gas diffusion layers (GDLs) and separator plates, which play a significant role in heat transfer. A parametric study is done to investigate the effect of various operating conditions on maximum cell temperature. The results are further validated with experiment. This model provides a theoretical foundation for thermal analysis of air-cooled stacks, where temperature non-uniformity is high and thermal management and stack cooling is a significant engineering challenge.

Keywords: PEM fuel cell; Air cooling; Thermal management; Forced convection; Heat transfer; Numerical modeling

1 Introduction

Fuel cells are devices that produce electricity through electrochemical reactions. In a proton exchange membrane fuel cell (PEMFC) oxidation and reduction half reactions are separated by a membrane. The fuel is hydrogen gas and the oxidant is ambient air or pure oxygen. The only byproducts of this reaction are heat and water. Regarding their high energy conversion efficiency, zero emission potential, low noise and potential use of renewable fuels, fuel cells are considered as future devices for mobile, stationary, and portable power applications. However, PEMFC systems are not currently cost effective; increasing their efficiency for transportation and stationary applications can improve their commercialization [1].

A simple way to improve the performance of a fuel cell is to operate the system at its maximum allowed temperature. At higher temperature, electrochemical activities increases and reaction takes place at a higher rate, which in turn increases efficiency. On the other hand, operating temperature affects the maximum theoretical voltage at which a fuel cell can operate. Higher temperature corresponds to lower theoretical maximum voltage and lower theoretical efficiency [2]. Temperature in the cell also influences cell humidity, which significantly influences membrane ionic conductivity. Therefore, temperature has an indirect influence on the cell output power through its impact on the membrane water content. The main purpose of thermal management in fuel cell systems is to ensure stack operation within a reliable temperature range. A detailed understanding of the stack thermal behaviour is therefore necessary for the selecting cooling solution. To analyze the

effectiveness of different thermal management strategies, developing a thermal model is essential. Oosterkamp [3] addressed some of the heat transfer issues for both PEM based systems and SOFC systems.

Many studies have been done on analytical and numerical modeling of PEMFCs. However, a few of them have concentrated on the area of thermal modeling and thermal management. Xue et al. [4] presented a zero-dimensional (lumped) dynamic model to investigate the mixed effects of temperature, gas flow, and capacitance, with emphasis on system transient behaviour. In their thermal model, only the convective heat transfer to the surrounding was considered. Shan and Choe [5] also considered one-dimensional temperature gradient across the fuel cell stack in through plane direction; they assumed that temperature is constant at each cell but varies from cell to cell.

There also exist several CFD based fuel cell models. For example, Pharoah and Burheim [6] presented a two-dimensional thermal model and obtained temperature distributions in a PEMFC in the plane normal to the cathode flow direction. In their work, only conductive heat transfer was considered. A three-dimensional model was developed by Shimpalee and Dutta [7], which solved the energy equation to predict the temperature distribution inside a straight channel PEMFC. They analyzed the effect of heat produced by the electrochemical reactions on the fuel cell performance. Adzakpa et al. [8] developed a three-dimensional dynamic model of a single cell to explain further phenomena such as the cell humidity and voltage degradations. Their heat transfer model included the conduction and heat generation inside the fuel cell and the convection on the outer surface. Convective heat transfer inside the fuel cell was not considered in the model of [8]. A comprehensive three-dimensional model that included analysis of species, heat, and charge transport in a single-channel unit cell, was presented by Sinha and Wang [9]. They investigated the performance of a PEMFC operating at high temperature. In their thermal model, a constant temperature condition was applied on all the external boundaries of the fuel cell. In the area of air-cooled fuel cells, Sasmito et al. [10] developed a two-dimensional numerical model to study the forced-air convection heat transfer in an open-cathode PEMFC. They considered two-phase flow and solved conservation equations of mass, momentum, species and energy in a single cell which represented a fuel cell stack by applying periodic boundary conditions.

In studying heat transfer during the operation of a PEMFC, the three-dimensional effects should be considered. However, the majority of the available numerical models are either not three-dimensional or are complex and involve high computational cost that makes it almost impossible to do parametric studies. In this paper, our focus is on air-cooled PEMFCs, in which forced convection heat transfer inside the stack plays an important role. A three-dimensional numerical study has been performed to investigate the effects of air velocity and bipolar plates thermal conductivity on the stack temperature. In the present thermal model, we have considered both conductive and convective heat transfer in addition to the heat generation inside a PEMFC stack to predict the temperature distribution. The results of this model is successfully validated by experimental data collected by Ballard Power Systems.

2 Model Development

Operation of a PEMFC is a complex process and includes transport of mass, momentum, energy, species and charges that take place simultaneously. Different parts of a PEMFC are comprised of current collectors, anode and cathode flow channels, GDLs, catalyst layers and the membrane. During the operation of a PEMFC, hydrogen molecules are supplied at the anode and split into protons and electrons. The polymeric membrane conducts protons to the cathode while the electrons are pushed round an external circuit and a current is generated from anode side to cathode side via electric load. Oxygen (form air) is consumed in the cathode side and reacts with the hydrogen ions, producing water and heat.

As mentioned above, PEMFC operation involves simultaneous, complex processes and hence, the development of three-dimensional models for a complete PEMFC that considers all parts, all components and transport phenomena is a major challenge. Furthermore, considering the whole fuel cell stack composed of several fuel cells as the computational domain, modeling multi-physics processes in a fuel cell system involves a significant computational cost, even by using high performance advanced numerical algorithms and taking advantage of parallel computing. One approach to overcome this problem is decoupling different processes by making simplifying assumptions that are reasonable and maintain the accuracy of the model. As an instance, when heat transport is the main interest of the analysis, we can skip solving equations of conservation of charge and species and instead, use the required input parameters from already existing models that capture other transport phenomena in a fuel cell.

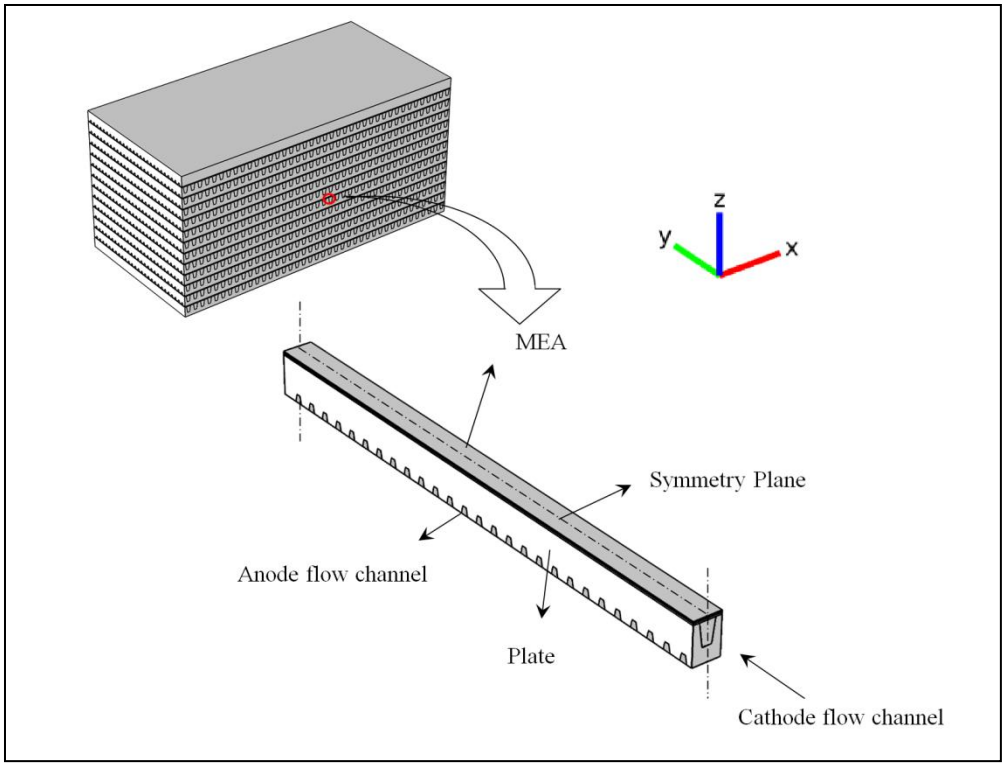

Figure 1: 3D schematic of a fuel cell stack and a cathode channel, the computational domain

In this study, the main goal is investigation of heat transfer in a PEMFC, in order to employ for developing new cooling strategies. Therefore a three-dimensional numerical study has been performed to analyze the effect of convective and conductive heat transfer on the stack temperature through parametric studies by varying the air velocity and bipolar plate thermal conductivity.

As explained previously, it is desirable to operate the fuel cell system at a temperature slightly below the maximum allowable temperature. Therefore, predicting the maximum temperature in a stack is of high importance. Heat transfer in a fuel cell stack includes: 1) natural convection from the outer surface of the stack to ambient air, 2) forced convection in the channels and porous layers, 3) conductive heat transfer in the solid phase, i.e. bipolar plates, GDLs, and catalyst coated membrane, and 4) radiation heat transfer from the stack surface.

Intuitively, one can predict that the maximum temperature occurs somewhere in the central cells of a fuel cell stack and the other cells that are closer to the outer surface experience a lower temperature as a result of heat transfer from the outer surface. Similarly, in a single cell we expect that the temperature in the central channel be higher than the other channels. Since one of the main interests of this research is to predict the maximum temperature in a stack, the complete stack is not modeled. Instead, we have considered the central cathode channel with plate and GDLs surrounding it in the central cell, which we expect have the maximum temperature in the whole stack. Taking advantage of symmetry in the fuel cell geometry, the computational domain is half of a single cathode channel as sketched in Figure 1.

Since air-cooled stack is studied here, we should include the air domain before entering the cathode channel and after exiting from the outlet. Otherwise, the heat transfer from the end sides cannot be accurately included in the model; even considering an equivalent convective heat transfer coefficient does not lead us to the same results as when we include the air domain in the inlet and outlet. A schematic of the computational domain including inlet and outlet air is shown in Figure 2.

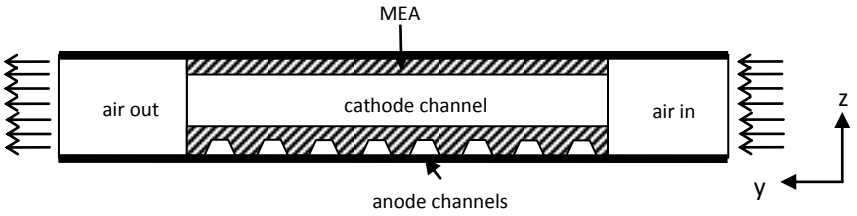

Figure 2: 2D schematic of the computational domain including ambient air before entering the channel and after exiting it; the dark lines on top and bottoms specify the periodic boundary condition.

In the present study, we have considered heat transfer in the entire domain and laminar flow in the oxidant channel. The convective heat transfer in the hydrogen channels and porous gas diffusion layers is negligible due to the relatively low velocity of fluid in these regions. Also, considering the central channel as the computational domain, it can be shown that radiation heat transfer is negligible since the temperature is not very high and also the surface area of the ends are small compared to the total surface area. The model inputs are current density, cell voltage, and inlet air flow temperature and velocity.

3 Governing Equations

For the solid region, heat transfer is through conduction. The governing equation is as follows:

$$\nabla.(k_s \nabla T_s) + \dot{q} = 0 \qquad \text{Eq. (1)}$$

where T_s is the temperature of the solid region. The heat is generated in the cathode catalyst layer.

In order to determine the amount of heat produced by a fuel cell, an energy balance for a fuel cell stack can be provided:

$$\sum_{\mathrm{i}} H_{i,in} = \sum_{\mathrm{i}} H_{i,out} + \dot{W}_{\mathrm{stack,gross}} + \dot{Q}_{\mathrm{total}} \qquad \text{Eq. (2)}$$

where $H_{i,in}$ and $H_{i,out}$ are the enthalpies of reactants and products respectively. The heat calculated using Equation (2) can be approximated by the following equation [12]:

$$\dot{Q}_{\mathrm{total}} = (E_{\mathrm{th}} - V_{\mathrm{cell}}) I n_{\mathrm{cell}} \qquad \text{Eq. (3)}$$

where V_{cell} is the voltage of the cell, I is the cell current, n_{cell} is the number of cells in a stack, and, E_{th} is the thermodynamic cell potential for a hydrogen/oxygen fuel cell, i.e., the maximum voltage obtained if the hydrogen heating value or enthalpy of formation were transformed into electrical energy, and is given by [1]:

$$E_{\mathrm{th}} = -\frac{\Delta H}{nF} \qquad \text{Eq. (4)}$$

Enthalpy of formation of water vapour at 25°C, $100\,kPa$ is $-241{,}826$ kJ/kmol. Therefore, if the lower heating value (LHV) is used, $E_{\mathrm{th}}(25°\mathrm{C}) = 1.253\,V$.

$\dot{Q}_{\mathrm{total}}$ must be transferred away from the cell to maintain the operating temperature of the fuel cell. It should be noted that by using the LHV, the implicit assumption is that all of the water produced in the cathode is in vapour form. This also means that the cooling effect of evaporation is implicitly included in heat production of Equation (3).

In this study, we derive V_{cell} and I from the experimental measurements. In future work, a performance model will be developed in order to be coupled with the current thermal model, from which V_{cell} and I can be calculated.

Due to symmetry, we have solved the equations in half of the domain. The symmetry boundary condition is applied on the side walls, which is equivalent to no heat flux in the normal direction across this boundary. Also periodic heat condition is applied on the top and bottom surfaces of the cell, where it contacts the adjacent cells in the stack. This boundary condition implies that $T(\text{at } z_{\min}) = T(\text{at } z_{\max})$ and also $\dot{q}_n(\text{at } z_{\min}) = \dot{q}_n(\text{at } z_{\max})$, see Figure 2.

For the fluid region, continuous, steady state, laminar (Re < 800), incompressible flow (Ma < 0.3) is assumed; therefore, the mass conservation, momentum principle, and energy equation are as follows

$$\nabla.(\rho\mathbf{u}) = 0 \qquad \text{Eq. (5)}$$

$$\rho\mathbf{u}\cdot\nabla\mathbf{u} = -\nabla p + \mu\nabla^2\mathbf{u} \qquad \text{Eq. (6)}$$

$$\rho c_p\mathbf{u}\,.\nabla T_f = \nabla.(k\nabla T_f) \qquad \text{Eq. (7)}$$

As the flow is continuous, we have no slip and no temperature jump over the wall. Therefore, the boundary condition for velocity field is u(at wall)$= 0$ and for temperature field is T (at wall) $= T_{\text{wall}}$. The flow enters with a constant uniform velocity, u_{in}, and constant temperature, T_{in}. For the fluid flow conditions at the outlet, no viscous stress along with constant pressure are considered, as follows,

$$\left(\mu(\nabla\mathbf{u} + (\nabla\mathbf{u})^T) - \frac{2}{3}\mu(\nabla\mathbf{u})\mathbf{I}\right)\mathbf{n} = 0,$$
$$p = p_{\text{atm}} \qquad \text{Eq. (8)}$$

where p_{atm} is the atmospheric pressure. This boundary condition is physically equivalent to the flow exiting into a large container. Note that because of the low velocity of hydrogen in the anode channels, we have neglected the convective heat transfer in anode side. Therefore, the only governing equation in anode channels is the same as Eq. (1). Also constant thermophysical properties have been assumed for solid phase while air properties such as density, heat capacity, and thermal conductivity vary with temperature. Air density is obtained from ideal gas law. The thermophysical properties used in the reference case are listed in Table 1.

Table 1. Thermophysical parameters used in the reference case.

$k_{\text{BP,thr}}$	20 W/m.K
$k_{\text{BP,in}}$	60 W/m.K
$k_{\text{GDL,in}}$	10 W/m.K
$k_{\text{GDL,thr}}$	0.7 W/m.K
k_{CCM}	1.5 W/m.K
k_{H_2}	0.18 W/m.K

4 Results and Discussion

For solving the system of partial differential equations explained in the previous section, we have used COMSOL Multiphysics 4.0a. Grid independency was checked by solving a case study using at first, ~0.6 million elements and then using ~2.3 million elements, which led to identical results. In this case study, which is our reference case, the inlet air velocity was 3.0 m/s, the inlet air temperature was 20℃, and the total heat generated in one cell, was 36W. Assuming 60 channels in one cell, the total heat generated in the domain was 0.3W. Figure 3 shows the temperature contours in the middle cross section of the channel. A uniform temperature distribution in the solid region is observed, whereas relatively high temperature gradient exists in the flow channel. Also in Figure 4 temperature contours are shown in different sections along the channel. For better description of temperature distribution in the solid and fluid regions, their temperature variations along x, y, and z directions are plotted in Figures 5 and 6. The horizontal axis shows the normalized location: $x/x_{\text{max}}, y/y_{\text{max}}, z/z_{\text{max}}$, where x_{max}, y_{max}, and z_{max}, specify the boundaries of the domain in x, y, and z.

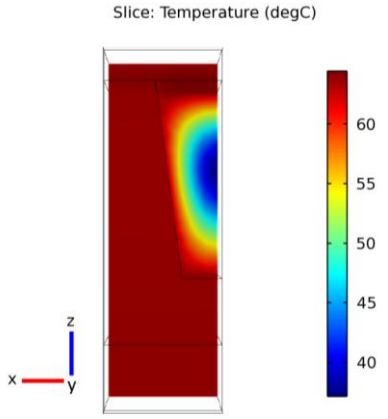

Figure 3: Temperature contours in the middle cross section of the channel (reference case).

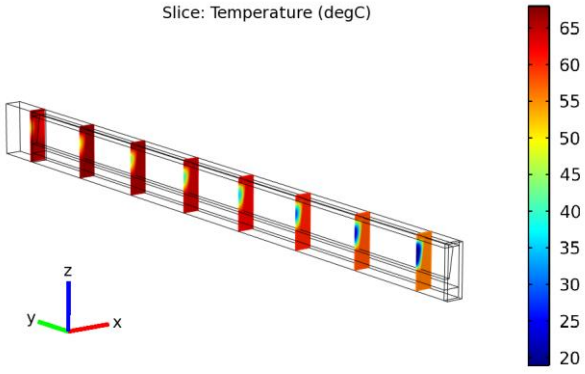

Figure 4: Temperature contours in eight slices from inlet to outlet of the channel (reference case).

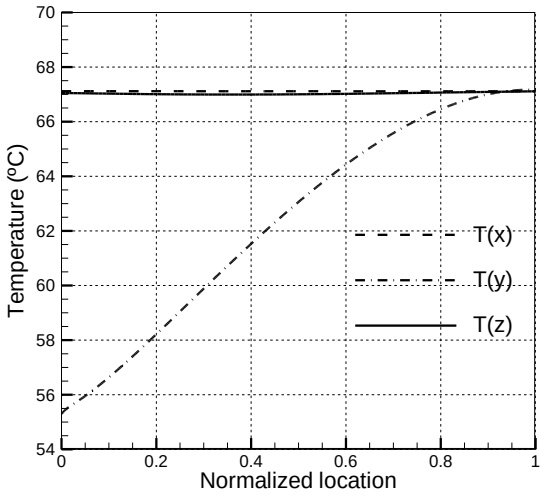

Figure 5: Temperature variation in different directions in bipolar plate (reference case).

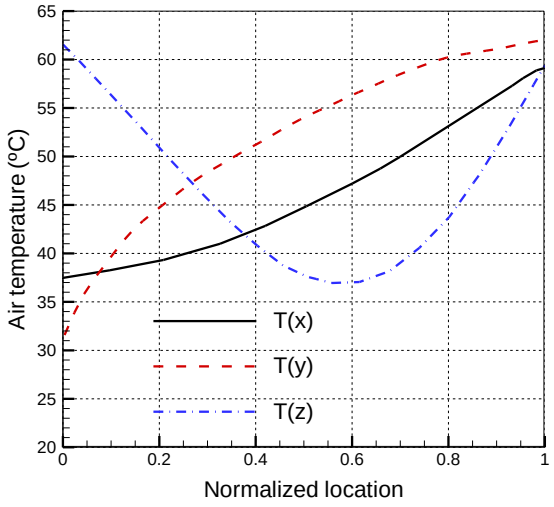

Figure 6: Temperature variation in different directions in air (reference case).

As previously mentioned, two major modes of heat transfer in this problem are forced convective heat transfer in cathode channels and conductive heat transfer in the entire domain. The average value of these two heat fluxes at different locations along the channel is calculated and plotted in Figure 7. As it can be inferred from this plot, the convective heat flux is two orders of magnitude higher than conductive heat flux. Moreover, the convective heat transfer almost remains constant along the channel, while in the same direction, conductive heat flux is decreasing. This is due to the different variation of the flow temperature gradient and the overall temperature gradient. In addition, conductive heat transfer is only changing by temperature gradient, which is decreasing; however, convective heat flux also depends on fluid density and velocity, which are not constant.

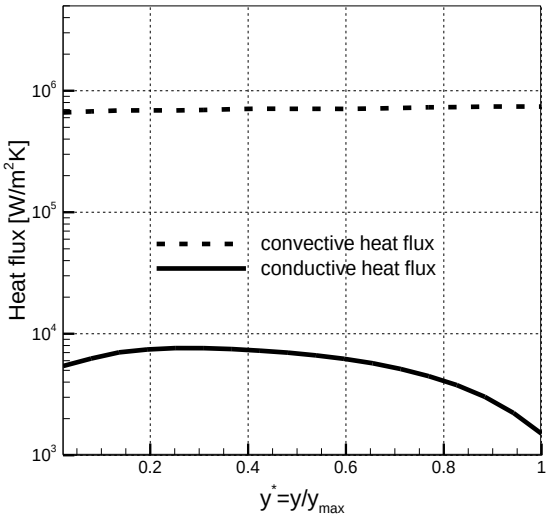

Figure 7: Mean conductive and convective heat flux in the direction of air flow (reference case)

For validating the present model, simulations under certain conditions have been performed and compared with experimental data provided by Ballard Power Systems for an air-cooled fuel cell stack consisting of 28 cells. The results are presented in Table 2. Here, the inlet air temperature is constant at room temperature while the air velocity and heat generation vary in different cases. The last column in this table shows the relative error between predicted maximum temperature and experimentally measured maximum temperature. The location of the experimental temperature measurement is the outlet of the central channel in the middle row of the stack.

In Table 3, the values of convective and conductive heat transfer are calculated using the following relations,

$$\dot{Q}_{\text{conv}} = \dot{m}_{\text{air}} c_p (T_{m,out} - T_{m,in})$$
$$\dot{Q}_{\text{cond}} = \dot{Q}_{\text{domain}} - \dot{Q}_{\text{conv}} \qquad \text{Eq. (9)}$$

where, $T_{m,in}$ and $T_{m,out}$ are the air mean temperatures calculated from Eq. (10), at the inlet and outlet of the channel, respectively.

Table 2. Model validation.

Test #	Air inlet temperature [°C]	Air inlet velocity, $u_{\text{in}}[\text{m/s}]$	Total heat generated in one cell, $\dot{Q}_{\text{cell}}$ [W]	Maximum temperature,$T_{\max}$[°C]		ΔT [°C]	$\frac{\Delta T}{T_{\text{sim}}}$
				Experiment*	Simulation	$T_{\text{sim}} - T_{\text{exp}}$	
1	21	2.19	37.7	65	68	3	4.4%
2	21	1.63	27.6	61	64	3	4.7%
3	21	1.45	29.1	67	69	2	2.8%
4	21	0.95	6.3	35	36	1	2.7%
5	21	0.94	13.7	50	54	4	7.4%

* Experimental results from Ballard Power Systems

Table 3. Comparison of conductive and convective heat transfer: all parameters are kept constant in different cases except the oxidant flow rate and k_{BP}

Case#	Air velocity $u_{in}[\text{m/s}]$	Plate thermal conductivity $k_{\text{BP}}[\text{W/ m.K}$	Total heat generated in the domain $\dot{Q}_{\text{domain}}[\text{W}]$	Convective heat transfer $\dot{Q}_{\text{conv}}[\text{W}]$	Conductive heat transfer $\dot{Q}_{\text{cond}}[\text{W}]$	Percentage of convective heat transfer	Percentage of conductive heat transfer
1	4.0	30	0.3	0.289	0.011	96%	4%
2	3.0	50	0.3	0.27	0.03	90%	10%
3	2.0	30	0.3	0.264	0.036	88%	12%
4	4.0	60	0.3	0.262	0.038	87%	13%

$$T_m = \frac{\int_{A_c} \rho u c_p T dA_c}{\dot{m}_{\text{air}} c_p} \qquad \text{Eq. (10)}$$

Also, the percentage of each type of heat transfer, under different conditions (air velocity and plate thermal conductivity), are compared in Table 3. In higher air velocities, convection is the major part of heat transfer, and the contribution of conductive heat transfer becomes more important as the plate thermal conductivity increases.

A parametric study has been performed to investigate the effect of air inlet velocity and plate thermal conductivity on the maximum temperature in the fuel cell stack. The results are plotted in Figures 8 and 9. In the parametric studies, only one parameter is variable and all other inputs parameters are the same as the reference case. By increasing the inlet air velocity or plate thermal conductivity, temperature drops considerably in the entire domain.

In Figure 10, effect of GDL thermal conductivity is investigated. It is obvious that unlike the plate thermal conductivity, which has significant impact on the temperature distribution, changing GDL thermal conductivity does not change the results (at least within the studied range).

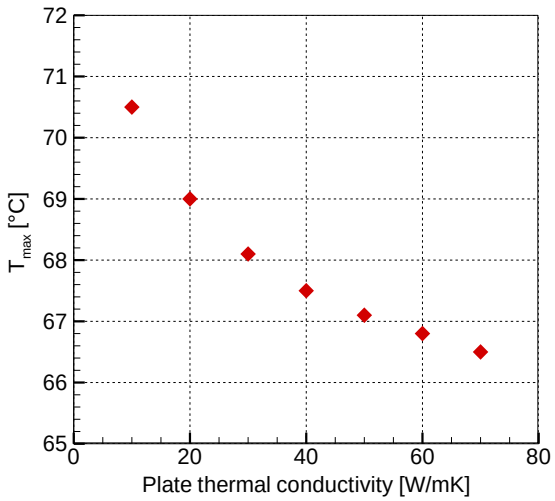

Figure 8: Effect of plate thermal conductivity on maximum temperature.

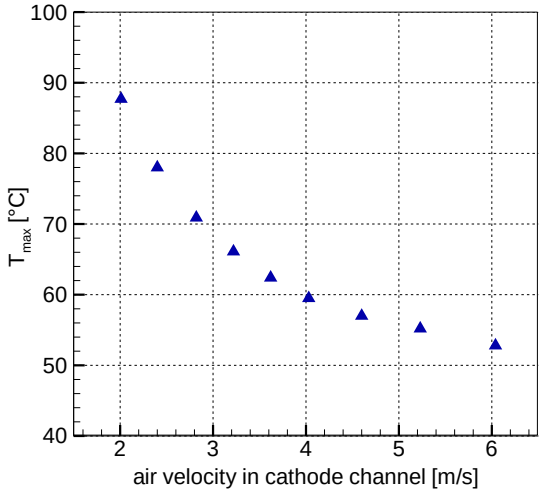

Figure 9: Effect of inlet air velocity on maximum temperature.

Also the effect of anisotropic GDL thermal conductivity is studied in Figure 11. In one case the in-plane and through plane thermal conductivities are 17 and 0.5 W/m.K respectively, and in the other case isotropic GDL was considered with thermal conductivity of 0.5 W/m.K.

Similarly, the effect of isotropic and anisotropic bipolar plate thermal conductivity is investigated and temperature distributions are plotted in Figure 12 for comparison. This Figure shows that the in-plane thermal conductivity of bipolar plate has more significant impact on the plate temperature distribution than the through-plane thermal conductivity. Using a higher thermal conductivity for bipolar plate leads to a more uniform temperature distribution in the plate.

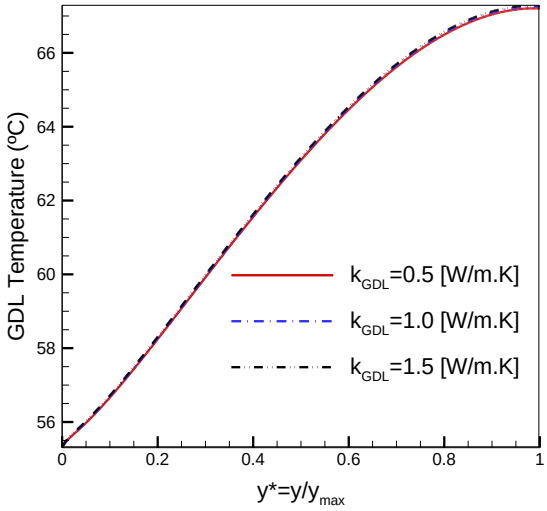

Figure 10: Effect of GDL thermal conductivity on GDL temperature distribution along the channel;

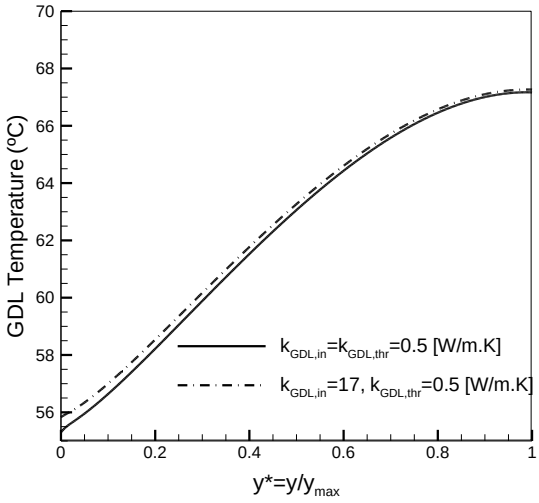

Figure 11: Effect of anisotropic GDL thermal conductivity on GDL temperature distribution along the channel.

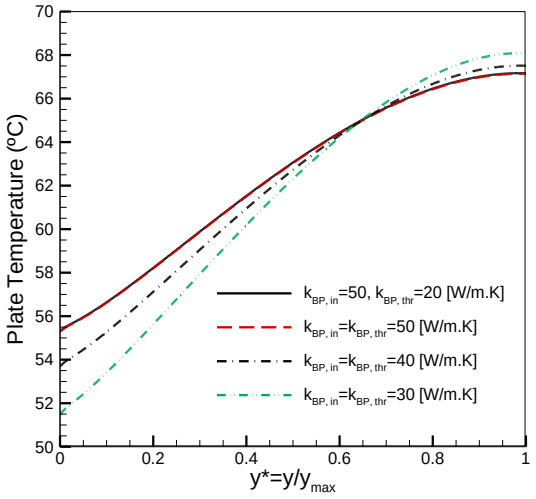

Figure 12: Effect of anisotropic bipolar plate thermal conductivity on temperature distribution along the channel.

5 Conclusions

In order to develop techniques and strategies for cooling and thermal management of PEMFCs, numerical modeling is a strong method that has been much considered in recent years. In the present work, a three-dimensional thermal model is developed to predict the temperature distribution in a PEMFC. The proposed model can be used for design and optimization of cooling devices for PEMFC systems. This model provides the maximum temperature in an air-cooled PEMFC stack, without considering the whole stack as the solution domain. The results show that the plate temperature gradient is much higher in the flow direction than any other direction. However, the oxidant temperature variation is considerable in all directions.

Moreover, different heat transfer regimes are analyzed, which reveals that in air-cooled fuel cell stacks, where the air velocity is high, the most significant heat transfer mode is the forced convective heat transfer. In fact, parametric studies show that the air velocity and bipolar plate thermal conductivity are among the critical factors that affect the temperature distribution in a PEMFC while the GDL thermal conductivity does not change the temperature profiles significantly. It should be noted that this conclusion is specific to the fuel cell stacks in which convective heat transfer is considerably higher than conductive heat transfer.

The validity of the model is verified by comparison of the results with experimental data, which shows a good agreement. In most of the cases, our model slightly overestimates the maximum temperature.

Possible reasons can be the insulated wall boundary condition assumption and uncertainty in thermophysical properties and also in approximating the heat generation term.

Acknowledgements
We would like to acknowledge Ballard Power Systems and Natural Sciences and Engineering Research Council of Canada, NSERC, for supporting this research.

List of Abbreviations and Variables

A_c	Cross-sectional area of the channel (m^2)
c_p	Specific heat ($J\ K^{-1}\ kg^{-1}$)
E_{th}	maximum voltage obtained from converting enthalpy of formation of hydrogen into electrical energy (V)
I	Electrical current
k	Thermal conductivity ($Wm^{-1}K^{-1}$)
$\dot{m}$	Mass flow rate (kgs^{-1})
$\mathbf{n}$	Outward unit normal
P	Pressure, (Pa)
PEM	Polymer electrolyte membrane fuel cell
$\dot{q}$	Heat generation (Wm^{-3})
$\dot{Q}$	Total heat generation (W)
T	Temperature (K)
u	Velocity (m/s)
$\mathbf{u}$	Velocity vector (m/s)
V_{cell}	output voltage of single fuel cell (V)

Greek symbols

μ	Fluid viscosity (N.s/m^2)
ρ	Density ($kg\ m^{-3}$)

Subscript

CCM	Catalyst coated membrane
cell	Single fuel cell
cond	Conduction
conv	Convection
domain	Domain
Exp	Experiment
f	Fluid
in	Inlet
m	Mean
max	Maximum
MEA	Membrane electrode assembly; contains two GDLs and a catalyst coated membrane
out	Outlet
BP	Bipolar plate
s	Solid
sim	Simulation

References

[1] J. Larminie, A. Dicks, Fuel Cell Systems Explained, John Wiley, 2002.

[2] A. Faghri, Z. Guo, Challenges and opportunities of thermal management issues related to fuel cell technology and modeling, International Journal of Heat and Mass Transfer, 48(19-20) (2005) 3891-3920.

[3] P.F. van den Oosterkamp, Critical issues in heat transfer for fuel cell systems, Energy Conversion and Management, 47 (2006) 3552–3561.

[4] X. Xue, J. Tang, A. Smirnova, R. England, N. Sammes, A hybrid multi-variable experimental model for a PEMFC, Journal of Power Sources, 133 (2004) 188–204.

[5] Y. Shan, S.-Y. Choe, A High Dynamic Fuel Cell Model with Temperature Effects, Journal of Power Sources 145 (2005) 30–39.

[6] J.G. Pharoah, O.S. Burheim, On the Temperature Distribution in Polymer Electrolyte Fuel Cells, Journal of Power Sources, 195 (2010), 5235-5245.

[7] S. Shimpalee, S. Dutta, Numerical prediction of temperature distribution in PEM fuel cells, Numerical Heat Transfer Part A, 38:111-128 , 2000

[8] Adzakpa, K.P. , Ramousse, J., Dub´e, Y., Akremi, H., Agbossou, K., Dostie, M., Poulin, A., Fournier, M., Transient Air Cooling Thermal Modeling of a PEM fuel cell, Journal of Power Sources 179 (2008) 164–176.

[9] P.K. Sinha and C.Y. Wang, Transport phenomena in elevated temperature PEM fuel cells, Journal of Electrochem Soc, 154 (2007), B106-116.

[10] A.P. Sasmito, K.W. Lum, E. Birgersson, A.S. Mujumdar, Computational study of forced-air convection in an open-cathode polymer electrolyte fuel cells stack. Journal of Power Sources, 195 (2010), 5550-5563.

[11] V.S. Arpaci, P.S. Larsen, Convection Heat Transfer, Prentice-Hall, Englewood Cliffs, NJ, 1984 (Chapter 4).

[12] J. Wishart, Z. Dong, and M. Secanell, Optimization of a PEM Fuel Cell System Based on Empirical Data and a Generalized Electrochemical Semi-Empirical Model, Journal of Power Sources, 161(2006), pp. 1041–1055.

[13] E. Sadeghi, N. Djilali, and M. Bahrami, Effective thermal conductivity and thermal contact resistance of gas diffusion layers in PEM fuel cells. Part 1: Effects of compressive load, J. Power Sources, 196 (2011), pp. 246-254.